Engineering Cytochrome *c* Peroxidase into Cytochrome P450: A Proximal Effect on Heme−Thiolate Ligation†

Jeffrey A. Sigman,‡ Alycen E. Pond,§ John H. Dawson,*,§,|| and Yi Lu*,‡

Department of Chemistry, University of Illinois at Urbana−Champaign, Urbana, Illinois 61801, Department of Chemistry and Biochemistry, University of South Carolina, Columbia, South Carolina 29208, and School of Medicine, University of South Carolina, Columbia, South Carolina 29208

Received April 8, 1999; Revised Manuscript Received June 7, 1999

ABSTRACT: In an effort to investigate factors required to stabilize heme−thiolate ligation, key structural components necessary to convert cytochrome *c* peroxidase (C*c*P) into a thiolate-ligated cytochrome P450-like enzyme have been evaluated and the H175C/D235L C*c*P double mutant has been engineered. The UV−visible absorption, magnetic circular dichroism (MCD) and electron paramagnetic resonance (EPR) spectra for the double mutant at pH 8.0 are reported herein. The close similarity between the spectra of ferric substrate-bound cytochrome P450cam and those of the exogenous ligand-free ferric state of the double mutant with all three techniques support the conclusion that the latter has a pentacoordinate, high-spin heme with thiolate ligation. Previous efforts to prepare a thiolate-ligated mutant of C*c*P with the H175C single mutant led to Cys oxidation to cysteic acid [Choudhury et al. (1994) *J. Biol. Chem. 267*, 25656−25659]. Therefore it is concluded that changing the proximal Asp235 residue to Leu is critical in forming a stable heme−thiolate ligation in the resting state of the enzyme. To further probe the versatility of the C*c*P double mutant as a ferric P450 model, hexacoordinate low-spin complexes have also been prepared. Addition of the neutral ligand imidazole or of the anionic ligand cyanide results in formation of hexacoordinate adducts that retain thiolate ligation as determined by spectral comparison to the analogous derivatives of ferric P450cam. The stability of these complexes and their similarity to the analogous forms of P450cam illustrates the potential of the H175C/D235L C*c*P double mutant as a model for ferric P450 enzymes. This study marks the first time a stable cyanoferric complex of a model P450 has been made and demonstrates the importance of the environment around the primary coordination ligands in stabilizing metal−ligand ligation.

Heme proteins are arguably the most versatile class of proteins in biology with their functions ranging from electron transfer to peroxide/oxygen activation to oxygen insertion (*1*, *2*). The diversity of function and spectroscopic characteristics of this class of proteins has largely been attributed to the structural components of the protein environment that constitute the heme active site, specifically the identity of the proximal axial ligand and residues located in the distal pocket. Cytochromes, globins, heme oxygenases, and the majority of peroxidases utilize His as the proximal ligand in either its neutral or deprotonated form. Catalases employ a Tyr phenolate axial ligand, while a Cys thiolate ligand is found in cytochrome P450 (*2*), *Caldariomyces fumago* chloroperoxidase (CPO)[1] (*3*), nitric oxide synthase (NOS) (*4*), and the carbon monoxide-sensing CooA protein (*5*). Biochemical, spectroscopic and X-ray crystallographic investigations of native enzymes, complemented by studies of inorganic model complexes, have greatly contributed to our understanding of the structure and function relationships within heme proteins.

Complementary to the above studies of native proteins, site-directed mutagenesis has allowed researchers to engineer mutant heme proteins as structural mimics for different heme proteins. This technique enables the researcher to alter the axial ligation of the protein in order to test principles obtained from earlier studies on the native protein and to determine key structural features governing the variability among protein functions. Examples of this approach can be seen for cytochrome b_5 (from His/His to His/Met) (*6*), cytochrome b_{562} (from His/Met to Met/Met) (*7*), cytochrome *c* (from His/

† This material is based upon work supported by the National Science Foundation under Award CHE 95-02421 to Y.L. (Career Award and Special Creativity Extension) and by National Institute of Health Grant GM 26730 to J.H.D. The electromagnet for the circular dichroism spectrophotometer was purchased through a grant from the Research Corporation. Y.L. is a Sloan Research Fellow of the Alfred Sloan Foundation, a Cottrell Scholar of the Research Corporation, a Camille Dreyfus Teacher−Scholar of the Camille and Henry Dreyfus Foundation, and a Beckman Young Investigator of the Arnold and Mabel Beckman Foundation.

* To whom correspondence should be addressed: Yi Lu, Phone (217)333-2619; Fax 217-333-2685; Email yi-lu@uiuc.edu. John H. Dawson, Phone, (803)777-7234; Fax (803)777-9521; Email dawson@psc.sc.edu.

‡ Department of Chemistry, University of Illinois at Urbana−Champaign.

§ Department of Chemistry and Biochemistry, University of South Carolina.

|| School of Medicine, University of South Carolina.

[1] Abbreviations: C*c*P, cytochrome *c* peroxidase; WTC*c*P, wild-type cytochrome *c* peroxidase; Mb, myoglobin; MCD, magnetic circular dichroism; EPR, electron paramagnetic resonance; CPO, chloroperoxidase; P450, cytochrome P450.

10.1021/bi990815o CCC: $18.00
Published on Web 07/31/1999

Met to His/Cys) (*8*), myoglobin (from His to Tyr or Cys) (*9*−*13*), or peroxidases (from His to Glu, Gln, or Cys) (*14*−*16*). Studies of these redesigned proteins demonstrate how altering the axial ligation of the heme can greatly affect the attributes of the protein. Further insight into the importance of the axial ligand has been gained by removing the proximal ligand altogether and replacing it with a noncoordinating Gly or Ala to generate cavity mutants. By adding various exogenous ligands into the cavity, researchers attempt to reconstitute wild-type enzyme activity (*17*−*22*) or to artificially mimic the activity of other heme systems.

Among all the axial ligands seen for heme proteins to date, thiolate ligation from Cys has received the most attention from researchers. This type of ligation has been shown to be important to both the reactivity and spectral characteristics of P450, NOS, CPO, and CooA (*2*−*5*). The strong electron donation from the thiolate to the iron is proposed to be responsible for heterolytic cleavage of the oxygen−oxygen bond, resulting in the high-valent active intermediate, compound I, which then can perform a variety of chemical reactions including hydroxylations, epoxidations, and dealkylations (*2*, *23*). The question of how the same thiolate−heme center performs different functions in various protein systems is extremely important yet remains largely unanswered. Introduction of a thiolate axial ligand into heme proteins that do not naturally possess this type of ligation could offer insight into this important question by monitoring the changes in structure, spectroscopic and functional properties following thiolate ligation. This strategy has been successfully employed in the myoglobin system with the H93C mutant, which compared favorably spectroscopically with cytochrome P450cam in the exogenous ligand-free ferric state (*9*−*11*).

Following the success of the myoglobin mutant, it is desirable to introduce thiolate ligation into a peroxidase system. The reasoning behind this choice is 2-fold. First, similar reaction intermediates (e.g., compounds I and II) are proposed in both peroxidases and P450 proteins (*23*) however, the lifetime and reactivity of those intermediates vary. Second, both the peroxidases and P450 proteins are capable of the peroxidase type electron-transfer reaction and the oxygen insertion reaction of P450. As the main difference between a peroxidase and a P450 protein is the ratio of electron transfer to oxygenation, or the branching ratio (*24*), the catalytic differences between the two types of proteins are more subtle than between myoglobin and P450. Successful introduction of thiolate ligation into a peroxidase system would allow investigators to probe the role of His and Cys in the catalytic activity of the peroxidase by comparing the structure and function of the two heme ligations in otherwise similar protein environments.

The active-site structures of P450 and cytochrome *c* peroxidase (C*c*P) are displayed in Figure 1 (*25*, *26*). As illustrated, the proximal cysteine ligand in P450 is in a hydrophobic environment provided by a conserved Phe residue. C*c*P, on the other hand, has a negatively charged residue, Asp235, in the analogous position with respect to the proximal ligand. Asp235 normally forms hydrogen bonds to the proximal His175 ligand in wild-type C*c*P (WTC*c*P) but might destabilize coordination of a negatively charged cysteine thiolate residue substituted for His175. Furthermore, previous efforts have shown that simply replacing His175 with Cys does not result in thiolate ligation (*15*). Replacement of Asp235 with a nonpolar amino acid in conjunction with the His175Cys mutation may help stabilize this interaction.

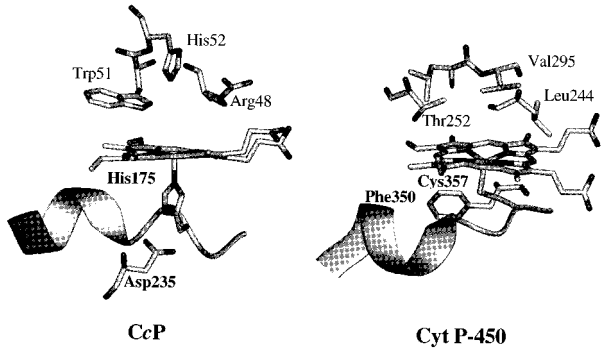

FIGURE 1: Active-site structures of WTC*c*P (*25*) and cytochrome P450cam (*26*).

In the present study, a H175C/D235L C*c*P double mutant has been engineered and characterized by UV−visible absorption, magnetic circular dichroism (MCD), and electron paramagnetic resonance (EPR) spectroscopy. Spectral analysis reveals that the C*c*P double mutant bears striking similarity to substrate-bound P450cam in both the resting ferric state and its imidazole and cyanide derivatives. The preparation of a stable ferric cyanide derivative marks the first time this derivative has been made in an engineered heme−thiolate protein and demonstrates the importance of the heme environment in stabilizing the thiolate ligation in both the pentacoordinate high-spin and hexacoordinate low-spin states of the heme.

EXPERIMENTAL PROCEDURES

Protein Sample Preparation. Construction, expression, and purification of C*c*P mutant proteins from *Escherichia coli.* were carried out as described previously (*27*), with the following modifications. A QuickChange site-directed mutagenesis kit (Stratagene, San Diego, CA) was used and the expressed protein was purified with 25 mM KH_2PO_4, pH 7.0, and 500 mM KCl containing 1 mM dithiothreitol (dithiothreitol was added to prevent disulfide formation) in the anion-exchange steps. The identity of the mutant was confirmed by DNA sequencing at the Genetic Engineering Facility at the University of Illinois. The homogeneity of the protein was confirmed by polyacrylamide gel electrophoresis. The mutation was further confirmed by electrospray mass spectrometry, which was performed at the University of Illinois mass spectrometry lab. The observed molecular mass for H175C/D235L C*c*P (33 699 Da) matches the calculated molecular mass (33 696 Da) within the allowed experimental error. Furthermore, these results confirmed that C175 in the mutant protein was not converted to cysteic acid upon reconstitution of the protein as previously seen with H175C C*c*P (*15*).

Spectroscopic Techniques. UV−visible absorption spectra were recorded on either a Hewlett-Packard 8453 UV−visible spectrometer or a Cary 210 spectrophotometer interfaced to an IBM PC. All UV−visible spectra were recorded with the protein in 100 mM potassium phosphate buffer and 50 mM KCl, pH 8.0, at 4 °C. The cell temperature was maintained with a circulating water bath equipped with a Polyscience digital temperature controller. For the titration experiments,

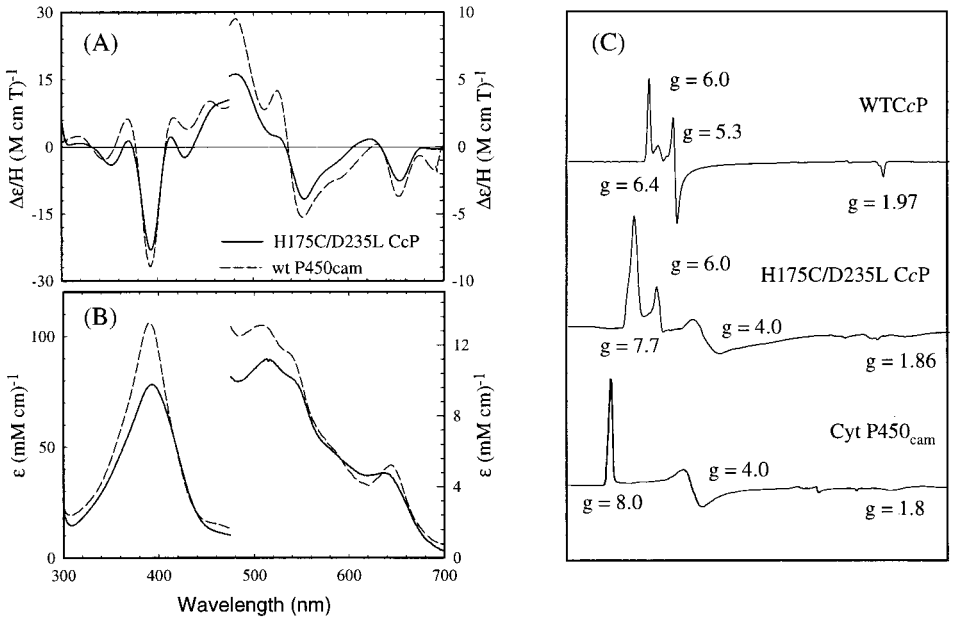

FIGURE 2: MCD (A) and UV−visible absorption (B) spectra of ferric H175C/D235L C*c*P (—) and cyt P450cam (- - -). For comparison purpose, the $\Delta\epsilon$/H values of ferric H175C/D235L C*c*P in the Soret region of MCD spectrum has been multiplied by 2. (C) X-band EPR spectra of the ferric forms of WTC*c*P (top), H175C/D235L C*c*P (middle), and cyt P450cam (bottom). The EPR spectrum of cyt P450cam is adapted from ref *63*. Refer to the Experimental Procedures section for conditions.

stock solutions of 5 M imidazole and 100 mM KCN were added to 2 mL of protein while stirring. Dissociation constants of imidazole and cyanide binding were determined from double-reciprocal plots of the change in absorbance versus concentration of substrate. The results are the average of three separate titrations from at least two wavelengths and with appropriate adjustments for dilution, which was less than 3%.

X-band EPR spectra were acquired on a Bruker ESP 300 equipped with a Oxford liquid helium cryostat and ITC4 temperature controller. Spectra were recorded on the samples in 100 mM potassium phosphate buffer at pH 7.0 for the wild-type C*c*P and pH 8.0 for H175C/D235L C*c*P. For wild-type C*c*P, 50% glycerol was used as a glassing agent. Glycerol seemed to disrupt the structure of the mutant, so 25% ethylene glycol was used instead. The spectra of ligand-free samples were recorded at 4 K with 10 mW power, and those of imidazole and cyanide derivatives were recorded at 20 K with 1 mW power.

MCD spectra were measured in a 0.2 cm cuvette at 1.41 T with a Jasco J500-A spectropolarimeter. This instrument was equipped with a Jasco MCD-1B electromagnet and interfaced with a Gateway 2000 4DX2-66V PC through a Jasco IF-500-2 interface unit. All spectral measurements were performed at ~4 °C, with data acquisition and manipulation being described elsewhere (*28*). UV−visible absorption spectra were recorded before and after the MCD measurements to verify sample integrity. The spectra of C*c*P presented here are overlaid with spectra of the ferric derivatives of P450cam that have been presented elsewhere (*29*−*31*) or recorded in this study. The MCD spectrum of ferric substrate bound P450 (*29*) closely resembles that of Vickery et al. (*32*).

RESULTS

The Ferric Enzyme. The MCD, UV−visible absorption, and EPR spectra of the ferric form of H175C/D235L C*c*P are shown in Figure 2. The spectra of substrate-bound ferric P450cam are included for comparison (*29*, *32*, *63*). Table 1 shows the absorbance peak maxima for the spectra in Figure 2B. As can be seen from Figure 2B and Table 1, the UV−visible absorption spectrum of the mutant has a Soret band at 392 nm, a second transition at 515 nm, and a charge-transfer band centered at 640 nm. These transitions translate in the MCD (Figure 2A) into a narrow trough in the Soret region centered at 392 nm and two troughs of unequal intensity at 555 and 656 nm in the visible region. These spectra are nearly identical to those of ferric camphor-bound P450cam in both the Soret and visible regions (*29*).

Table 1: Spectral Properties of Selected Heme Proteins and Ligand Complexes

protein	δ	Soret	β	α	CT	reference
Ferric Ligand Free						
H175C/D235L C*c*P		392	515		640	this work
P450cam		391	515		646	*61*
CPO		396	515		650	*62*
WTC*c*P		408	509		646	this work
Ferric Imidazole						
H175C/D235L C*c*P	360	422	542	565	648, 748	this work
P450cam	360	425	541	578		*30*
CPO	360	429	546	580	640	*36*
WTC*c*P		412	536	563		this work
Ferric Cyanide						
H175C/D235L C*c*P	368	437	558	591	800	this work
P450cam	364	438	558			*36*
CPO	365	439	557	594		*36*
human Mb(H93C)		421	550			*9*
human Mb		422	541			*9*
WTC*c*P	360	420	542	568		this work

The ferric C*c*P double mutant has a high-spin rhombic EPR signal (Figure 2C; see Table 2 for summary) analogous to the spectra of ferric P450cam and CPO with *g*-values at 7.7, 4.0, and 1.8 (*33*, *34*). A small axial component is also observed in the spectra, which may be due to the disruption

Table 2: X-Band EPR Parameters of Selected Heme Proteins and Ligand Complexes

protein	*g*-values	reference
Ferric		
H175C/D235L C*c*P	7.7, 4.0, 1.8	this study
P450	7.9, 4.0, 1.8	33
CPO	7.6, 4.3, 1.8	*34*
human Mb (H93C)	8.4, 3.2, 1.6	*10*
WTC*c*P	6.4, 5.3, 2.0	this study
Ferric Imidazole		
H175C/D235L C*c*P	2.45, 2.28, 1.91	this study
P450	2.56, 2.27, 1.87	33
CPO	2.53, 2.28, 1.85	*38*
WTC*c*P + (SCH_2CH_2OH)	2.46, 2.26, 1.91	this study
Ferric Cyanide		
H175C/D235L C*c*P	2.52, 2.30, 1.85	this study
P450	2.45, 2.28, 1.83	*33*
CPO	2.66, 2.31, 1.77	*38*
WTC*c*P	3.30, 2.00, - - -	this study

of protein structure upon freezing or possibly from damaged or denatured protein. A freezing effect has been observed in native C*c*P but is eliminated if the protein is frozen in the presence of glycerol (*35*). However, glycerol seems to disrupt the structure of the mutant causing an increase of the axial signal at the expense of the rhombic signal. To avoid this effect, ethylene glycol was substituted for glycerol as a glassing agent.

Imidazole Complex of Ferric H175C/D235L CcP. To further probe the heme environment and the stability of the axial Cys ligand, the spectra of the ferric C*c*P double mutant in the presence of exogenous ligands have been analyzed. Titration of the mutant or WTC*c*P with imidazole resulted in changes in the UV−visible absorption spectrum indicative of conversion of the heme iron from high to low spin (Supporting Information). Clean isosbestic points in the spectra indicated that no intermediates were formed during the process. The double-reciprocal plot of the change in ligand concentration versus the change in absorption at 423 nm (413 nm for WTC*c*P) results in a linear least-squares fit of the data points of a straight line ($R^2 \geq 0.99$), giving a dissociation constant of 40 mM (Supporting Information). This value suggests a slightly weaker binding affinity for imidazole than that of wild-type C*c*P ($K_D = 20$ mM) but stronger than for imidazole binding to CPO ($K_D = 250$ mM) (*36*), a thiolate-ligated peroxidase.

The MCD and UV−visible absorption spectra of the imidazole adduct of the double mutant and of P450cam (*31*) are shown in Figure 3, panels A and B, respectively, with the peak maxima for the absorption data summarized in Table 1. The imidazole complex of the H175C/D235L C*c*P mutant has a Soret absorption band at 422 nm, a second peak at 542 nm and a shoulder at 565 nm. These transitions give rise to the MCD spectrum seen in Figure 3A, which shows a derivative-shaped feature centered at 420 nm and a set of overlapping derivative-shaped patterns in the visible region with minima at 550 and 582 nm.

The EPR spectrum of the imidazole-bound ferric C*c*P double mutant is compared to that of wild-type C*c*P with β-mercaptoethanol in Figure 3C. The ligands to the heme should be similar for both systems, each with a thiolate ligand trans to the imidazole (or His) ligand. The similarity of the spectra and the nearly identical sets of *g*-values (2.45, 2.28, and 1.91 for the imidazole complex of the ferric mutant and 2.46, 2.26, and 1.91 for the β-mercaptoethanol complex of wild-type C*c*P) can be seen in Figure 3C and in Table 2.

Cyanide Adduct of Ferric H175C/D235L CcP. Titrations of the ferric double mutant with cyanide resulted in replacement of the Soret transition at 392 nm with one at 437 nm (Supporting Information). The double-reciprocal plot of the change in ligand concentration versus the change in absorption at 437 nm gave a least-squares fit that was linear with $R^2 \geq 0.99$ (Supporting Information). From the plot, a dissociation constant of 0.09 mM was obtained, which indicates significantly weaker binding of CN^- to the mutant than to the wild-type C*c*P ($K_D = 0.001$ mM) (*37*) or to CPO ($K_D = 0.018$ mM) (*36*). This result is consistent with thiolate coordinating to the heme iron in the cyanide derivative of the mutant, as the thiolate has a stronger trans effect on cyanide binding than the imidazole in ferric wild-type C*c*P.

A comparison of MCD and UV−visible spectra of the cyanide-bound ferric C*c*P double mutant with that of ferric P450cam−cyanide (*31*) is illustrated in Figure 4 and Table 1. The C*c*P double mutant exhibits Soret, β, and α bands at 437, 558, and 591 nm, respectively, which are nearly identical to those of the cyanoferric complexes of P450 and CPO (*31*, *36*). The MCD spectra (Figure 4A) further substantiate this similarity with a derivative-shaped feature centered at 436 nm and a single trough at 584 nm in the visible region, both of which are also seen in the spectrum for the analogous complex of P450cam (*31*).

EPR spectra of the mutant and wild-type C*c*P with cyanide are compared in Figure 4C and the *g*-values are shown in Table 2. The mutant has an EPR spectrum that is identical to that of P450 (*33*) and CPO (*38*) with narrowly spaced *g*-values at 2.52, 2.30, and 1.85, indicating that Cys175 remains ligated when the mutant binds the negatively charged cyanide ligand.

DISCUSSION

Cytochrome P450 has been the focus of research for several decades because of its unique spectroscopic properties and the variety of useful chemical transformations it performs that are important in both biological function and chemical synthesis (*2*). An important milestone in this field of research was the synthesis of model porphyrin compounds that accurately reproduced the spectral properties of P450 (*39*−*41*). These models complement the study of native enzymes and provide insight into the key structural elements that define the spectroscopic properties and reaction mechanism of the enzyme. This accomplishment has recently been repeated with engineered mutants of human and horse heart myoglobin by Adachi et al. (*9*, *10*) and Hildebrand et al. (*11*), respectively, that spectroscopically resembled ferric P450. Making a P450 mimic from a His-ligated peroxidase, however, has proven to be more difficult.

To date, successful introduction of a Cys proximal ligand into a peroxidase has not been reported. Choudhury et al. (*15*) mutated the proximal His175 of C*c*P to Cys, but this experiment did not result in thiolate ligation to the heme. Instead, they determined by X-ray crystallography that the proximal Cys had been oxidized to cysteic acid. It was suggested that this had occurred due to the smaller size of

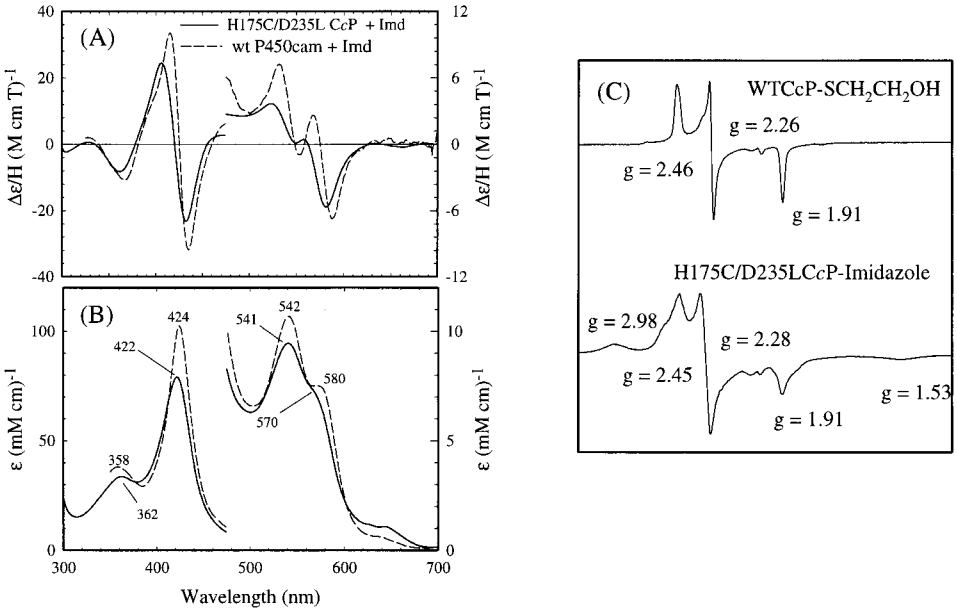

FIGURE 3: MCD (A) and UV−visible absorption (B) spectra of the ferric imidazole derivatives of H175C/D235L C*c*P (—) and cyt P450cam (- - -). (C) X-band EPR spectra of the ferric β-mercaptoethanol derivative of WTC*c*P (top) and the ferric imidazole derivative H175C/D235L C*c*P (bottom). Refer to the Experimental Procedures section for conditions.

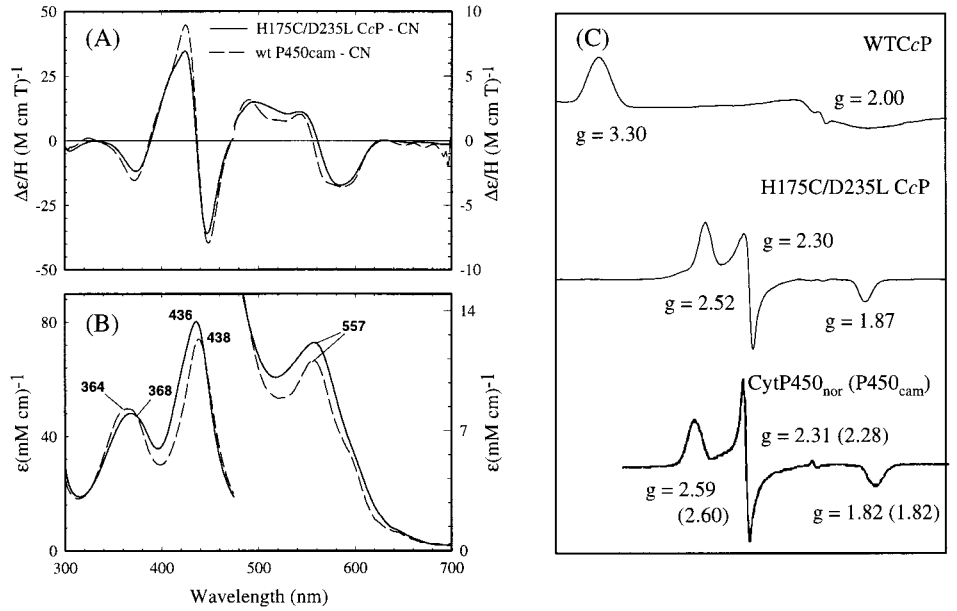

FIGURE 4: MCD (A) and UV−visible absorption (B) spectra of the ferric cyanide derivatives of H175C/D235L C*c*P (—) and cyt P450cam (- - -). (C) X-band EPR spectra of the ferric cyanide derivatives of WTC*c*P (top), H175C/D235L C*c*P (middle), and cyt P450cam (bottom). The EPR spectrum of cyt P450cam is adapted from refs *33* and *64*. Refer to the Experimental Procedures section for conditions.

Cys relative to His, presumably leaving the Cys too far from the heme iron to bind properly and susceptible to oxidation.

To test the proposal that thiolate ligation failed in H175C C*c*P due to the longer distance of the Cys to the heme iron, we designed a triple mutant, A174G/H175C/L177G C*c*P, to disrupt the helix and allow the proximal Cys to reach the heme iron. Spectroscopic characterization of this mutant was again inconsistent with Cys ligation (data not shown). Therefore, either the mutation did not result in a relaxed structure that would allow Cys to reach the heme iron or other structural elements within the heme environment are important for successful thiolate ligation. As illustrated by a distal effect in horse heart myoglobin, in which mutating the distal H64 to a Val permitted the proximal Cys to bind to the heme iron in the H64V/H93C double mutant (*11*), the surrounding protein can play a significant role in axial ligand binding and stability.

A recent review on the role of axial ligands stressed the importance of the local structural and electronic environment around the proximal ligand (*23*, *42*, *43*). For example, it was proposed that thiolate ligation in P450 and CPO is stabilized by the location of the Cys at the positive end of a helix dipole and by hydrogen-bond donation from backbone amide groups to the thiolate sulfur atoms (*25*, *26*, *44*, *45*). Crystallographic studies of C*c*P, P450cam, and CPO reveal several differences in the environment around their proximal ligands (*25*, *26*, *44*). In both thiolate-ligated proteins, a nonpolar amino acid (Phe in P450cam and Leu in CPO) and the protein backbone

form an enclosure about the proximal Cys ligand. This nonpolar residue is conserved in several P450 proteins and is observed at the same position in the crystal structures of three other P450 enzymes (*46*−*48*). In contrast, the analogous amino acid in C*c*P is Asp (D235, Figure 1). This residue accepts a hydrogen bond from the proximal His, giving it more imidazolate character and contributing to the more negatively charged proximal environment in C*c*P (*25*, *49*). Previous D235 mutants have changed the spectroscopic and redox properties of C*c*P through interactions with H175 (*49*).

On the basis of the above considerations, the mutation of D235 to Leu has been made in addition to the H175C mutation, resulting in the H175C/D235L C*c*P double mutant. The mutation of Asp to Leu was chosen because Leu is nonpolar but similar in shape to Asp. This change should relieve the conflict between the negative charges of the Asp and Cys residues and provide a similar hydrophobic environment for the thiolate ligand in this engineered C*c*P as in P450. The second mutation may also provide some steric push to bring the Cys closer to the heme iron. There must be some movement of the Cys toward the heme since the Fe−S(Cys) distance in the H175C single mutant is about 4.3 Å (*15*). Furthermore, since Asp235 plays a crucial role in the proximal H-bond network in C*c*P, one cannot rule out possible contributions from other proximal residues in the structural changes leading to the coordination of Cys175. The MCD, UV−visible absorption, and EPR studies of the C*c*P double mutant and of its imidazole and cyanide adducts reported herein conclusively prove that Cys is ligated to the heme iron. Clearly, the D235L mutation is crucial in promoting Cys ligation to the C*c*P heme iron in the double mutant.

The presence of a Soret transition near 390 nm in the UV−visible absorption spectrum of the ferric mutant and the similarity of its MCD spectrum to that of ferric substrate-bound P450cam (Figure 2A,B) substantiates assignment of the C*c*P double mutant as a thiolate-ligated pentacoordinate high-spin complex. Further evidence for stable thiolate ligation in the C*c*P double mutant comes from the large rhombic splitting observed in the EPR spectrum of the high-spin state (Figure 2C). A distinguishing characteristic of pentacoordinate high-spin ferric thiolate-bound heme proteins such as P450cam and CPO is the display of g_x, g_y, and g_z values in the range of 7−8, 3−4, and ∼1.8, respectively (*34*, *39*, *41*, *50*−*52*, *63*) (see Table 2). The observation that the ferric double mutant is pentacoordinate contrasts with the previously examined proximal ligand mutants of C*c*P (H175E and H175N), which are hexacoordinate at neutral pH (*14*, *15*). For the ferric C*c*P double mutant, the Soret absorption peak is independent of pH between 8.0 and 6.5, and then begins to blue-shift as the pH is lowered further (data not shown). Conversely, the H175E, H175N, and H175C proximal ligand mutants of ferric C*c*P all become unstable at pH values above 6.5 and exhibit a large decrease in their Soret maxima, indicating either the loss of the heme prosthetic group or significant destabilization of the heme pocket (*15*).

The role of the proximal environment in the support of Cys ligation has not been evaluated in the H93C Mb models. Hildebrand et al. (*11*) determined that an additional mutation in the *distal* pocket of horse heart Mb (H64V) was necessary to produce a mutant Mb that displayed spectroscopic properties similar to those of ferric P450. The nonpolar distal side chain of Val was believed to cause the iron to move toward the proximal heme side in conjunction with some structural changes that allowed Cys to bind. Movement of iron below the plane of the heme is not likely to play much of a factor in the observed stability of thiolate ligation in the H175C/D235L C*c*P mutant since the C175 remains bound even when a sixth ligand is present and the iron is believed to be in the plane of the heme. Therefore the D235L mutation must allow C175 to move closer to the heme iron in addition to the previously discussed electrostatic or hydrophobic effects.

The UV−visible absorption data for the imidazole complex of the C*c*P double mutant (Figure 3B) supports the retention of thiolate ligation in the hexacoordinate state. The position of the Soret band is 422 nm, similar to that seen in the spectrum of the analogous form of P450cam (see Table 1). In contrast, the imidazole adduct of wild-type C*c*P exhibits a Soret band 10 nm blue-shifted to 412 nm, typical of bis(imidazole) ligation as in cytochrome b_5 (*53*, *54*). Furthermore, the spectrum of ferric H175C/D235L C*c*P has bands at 648 and 748 nm which have also been observed in P450−imidazole complexes (*55*) and more recently in the CO-sensing enzyme CooA, a new heme protein with a His−Fe(III)−Cys heme coordination environment (*5*, *56*). These bands have been assigned to thiolate sulfur to heme iron charge-transfer transitions (*8*, *55*). The comparison of the MCD spectra of the imidazole complexes of ferric H175C/D235L C*c*P and of P450cam seen in Figure 3A offers supporting evidence to the coordination assignment based on the UV−visible data. The close match in band shape in both the Soret and visible regions of the MCD spectra indicates a similarity in coordination structure. Comparison of the MCD spectrum of the C*c*P double mutant with the spectrum of ferric cytochrome b_5 (data not shown) confirms the spectral difference between a bis(imidazole) (cyt b_5) and a imidazole/cysteine (H175C/D235L C*c*P) coordination. However, the lack of intensity of both the derivative in the Soret region and the two troughs in the visible region of the MCD spectrum of the mutant indicate that a second minor species may be present, most likely a bis(imidazole) form. The narrow range of *g*-values observed in the EPR spectrum of the double mutant (Figure 3C) is also characteristic of low-spin thiolate-ligated proteins (*34*, *38*, *39*, *50*, *51*, *57*). EPR spectra of cytochrome b_5 or the imidazole complex of ferric myoglobin, for comparison, have more widely dispersed *g*-values at ∼3.0, ∼2.1, and ∼1.5 (*58*). The spectrum of the double mutant also differs from the low-spin EPR spectrum of WTC*c*P (g = 2.7, 2.2, and 1.78), which has been attributed to a freezing-induced coordination of either hydroxide or the distal His residue (*35*). A minor portion of the sample displays a set of bis(imidazole) signals at *g*-values 2.98 and 1.53 that is most likely due to displacement of the Cys ligand by imidazole in conjunction with the binding of imidazole from His52 on the distal side, confirming the findings seen in the MCD spectrum. Nonetheless, the spectral similarities between the mutant and P450cam for all three spectroscopic techniques represent strong evidence for a similar heme environment, imidazole−Fe(III)−Cys, as the major species in the ferric double mutant.

As cyanide is a stronger ligand to heme iron than imidazole, and also possesses a negative charge, attempts at preparing a cyanoferric derivative of either porphyrin P450

model compounds or H93C Mb failed (*9*). This can be attributed to competition between the negative charges of cyanide and thiolate, apparently leading to thiolate dissociation. Interestingly, H93C Mb has a peptide carbonyl in the analogous position to Asp235 in C*c*P. The carbonyl oxygen is polar but does not possess a full negative charge like Asp, which may explain why the ligation of cysteine was stable in the five-coordinate state but not in the cyanoferric derivative of the Mb mutant. In contrast to the H93C Mb case, thiolate ligation is retained in the ferric H175C/D235L C*c*P system following the addition of exogenous cyanide. Comparison of the UV−visible absorption and MCD data of the cyanoferric C*c*P mutant to those of the analogous state of P450cam (Figure 4A,B), specifically the location of the Soret absorption peak at 436 nm, demonstrate that thiolate ligation is retained in this derivative of the C*c*P mutant. The UV−visible absorption spectrum of the C*c*P mutant is quite different from those of the cyanoferric derivatives of wild-type C*c*P, as well as ferric H93C Mb (see Table 1), which both have Soret absorption maxima at ∼420 nm and visible peaks at ∼540 nm (*9*), indicating cyanide−Fe(III)−histidine ligation. The close similarity between the EPR spectra of the cyanoferric derivatives of the double mutant and of P450cam (Figure 4C, Table 2) lends further support to the ligation assignment of Cys−Fe(III)−CN. Conversely, wild-type cyanoferric C*c*P has widely spaced *g*-values similar to the cyanoferric derivatives of other heme proteins with proximal His ligands such as horseradish peroxidase (*59*).

The successful formation of a cyanoferric complex that maintains thiolate ligation in our double mutant is attributable to a combination of steric, electrostatic, and hydrophobic effects of the Asp235Leu mutation. The same effects may play a role stabilizing the cyanoferric complex of P450 because Phe350 is at the corresponding position in P450cam. However, these effects by Aps235Leu mutation were apparently not enough to stabilize thiolate-bound ferrous or ferrous CO forms of the C*c*P double mutant because our preliminary study indicates that Cys is not retained as the axial ligand in these derivatives. Attempts to reoxidize the reduced protein yielded a sample whose spectrum did not match that of the original oxidized protein. Furthermore, mass spectrometry indicated that, after reduction and workup in the presence of dioxygen, a portion of the sample had increased in molecular weight by ∼32 mass units. This is consistent with oxidation of the cysteine under these conditions. The overall charge on the heme unit in both the deoxyferrous and cyanoferric states is the same. Thus, it is probably not the overall charge but the low affinity of thiolate for ferrous iron that causes the loss of the axial Cys upon reduction of the mutants. This low affinity has been compared to the low binding affinity of cyanide for ferrous porphyrins caused by the repulsion between the high electron density on the iron and the negatively charged cyanide (*60*). Previous studies in ferrous thiolate heme models have shown that thiolate binding to the ferrous state could only be stabilized through the use of strong base or crown ether complexes of the thiolate ligand (*60*). This is not possible in proteins, however. Instead, both P450 and CPO utilize peptide amide N−H groups to hydrogen-bond to the thiolate sulfur to decrease the charge density on this ligand (*42*). Additional mutations that are in appropriate positions to hydrogen-bond C175 and stabilize the Cys in the ferrous state are in progress and will be reported in the future.

In summary, the mutation of D235 to Leu is necessary for stabilization of thiolate ligation in ferric H175C C*c*P. Spectral comparison of the ferric, ferric imidazole, and ferric cyanide forms of H175C/D235L C*c*P by UV−visible absorption, MCD, and EPR spectroscopies to the analogous adducts of P450cam substantiate the retention of thiolate ligation in the presence of neutral and anionic ligands. Therefore, H175C/D235L C*c*P represents the first example of stable thiolate ligation within a peroxidase system. This study marks the first time a stable cyanoferric complex of a model P450 has been made and demonstrates the importance of the environment around the primary coordination ligands in stabilizing metal−ligand ligation.

ACKNOWLEDGMENT

We thank Wilson King and Brian Kwok for help in protein preparation, Alan Gengenbach and Drs. Stephen G. Sligar, Kenneth S. Suslick, Masanori Sono, and Amy P. Ledbetter for helpful discussions, and Drs. Edmund Svastis and John J. Rux for assembling the MCD software.

SUPPORTING INFORMATION AVAILABLE

Three figures showing UV−visible absorption titrations of ferric WTC*c*P and (H175G/D235L) C*c*P with imidazole and ferric (H175G/D235L) C*c*P with cyanide and the resulting double-reciprocal plots. This material is available free of charge via the Internet at http://pubs.acs.org.

REFERENCES

1. Bertini, I., Gray, H. B., Lippard, S. J., and Valentine, J. S. (1994) *Bioinorganic Chemistry*, University Science Books, Sausalito, CA.
2. Sono, M., Roach, M. P., Coulter, E. D., and Dawson, J. H. (1996) *Chem. Rev. 96*, 2841−2887.
3. Erman, J. E., Hager, L. P., and Sligar, S. G. (1994) *Adv. Inorg. Biochem. 10*, 71−118.
4. Sono, M., Stuehr, D. J., Ikada-Saito, M., and Dawson, J. H. (1995) *J. Biol. Chem. 270*, 19943−19948.
5. Shelver, D., Thorsteinsson, M. V., Kerby, R. L., Chung, S. Y., Roberts, G. P., Reynolds, M. F., Parks, R. B., and Burstyn, J. N. (1999) *Biochemistry 38*, 2669−2678.
6. Sligar, S. G., Egeberg, K. D., Sage, J. T., Morikis, D., and Champion, P. M. (1987) *J. Am. Chem. Soc. 109*, 7896−7897.
7. Barker, P. D., Nerou, E. P., Cheesman, M. R., Thomson, A. J., de Oliveira, P., and Hill, H. A. O. (1996) *Biochemistry 35*, 13618−13626.
8. Raphael, A. L., and Gray, H. B. (1991) *J. Am. Chem. Soc. 113*, 1038−1040.
9. Adachi, S.-i., Nagano, S., Watanabe, Y., Ishimori, K., and Morishima, I. (1991) *Biochem. Biophys. Res. Commun. 180*, 138−144.
10. Adachi, S.-i., Nagano, S., Ishimori, K., Watanabe, Y., Morishima, I., Egawa, T., Kitagawa, T., and Makino, R. (1993) *Biochemistry 32*, 241−252.
11. Hildebrand, D. P., Ferrer, J. C., Tang, H.-L., Smith, M., and Mauk, A. G. (1995) *Biochemistry 34*, 11598−11605.
12. Hildebrand, D. P., Burk, D. L., Maurus, R., Ferrer, J. C., Brayer, G. D., and Mauk, A. G. (1995) *Biochemistry 34*, 1997−2005.
13. Matsui, T., Nagano, S., Ishimori, K., Watanabe, Y., and Morishima, I. (1996) *Biochemistry 35*, 13118−13124.
14. Choudhury, K., Sundaramoorthy, M., Mauro, J. M., and Poulos, T. L. (1992) *J. Biol. Chem. 267*, 25656−25659.
15. Choudhury, K., Sundaramoorthy, M., Hickman, A., Yonetani, T., Woehl, E., Dunn, M. F., and Poulos, T. L. (1994) *J. Biol. Chem. 269*, 20239−20249.

16. Smulevich, G., Neri, F., Willemsen, O., Choudhury, K., Marzocchi, M. P., and Poulos, T. L. (1995) *Biochemistry 34*, 13485−13490.
17. Lu, Y., Casimiro, D. R., Bren, K. L., Richards, J. H., and Gray, H. B. (1993) *Proc. Natl. Acad. Sci. U.S.A. 90*, 11456−11459.
18. DePillis, G. D., Decatur, S. M., Barrick, D., and Boxer, S. G. (1994) *J. Am. Chem. Soc. 116*, 6981−6982.
19. Barrick, D. (1994) *Biochemistry 33*, 6546−6554.
20. McRee, D. E., Jensen, G. M., Fitzgerald, M. M., Siegel, H. A., and Goodin, D. B. (1994) *Proc. Natl. Acad. Sci. U.S.A. 91*, 12847−12851.
21. Wilks, A., Sun, J., Loehr, T. M., and Ortiz de Montellano, P. R. (1995) *J. Am. Chem. Soc. 117*, 2925−2926.
22. Newmyer, S. L., Sun, J., Loehr, T. M., and Ortiz de Montellano, P. R. (1996) *Biochemistry 35*, 12788−12795.
23. Dawson, J. (1988) *Science 240*, 433−439.
24. Rietjens, I. M. C. M., Osman, A. M., Veeger, C., Zakharieva, O., Antony, J., Grodzicki, M., and Trautwein, A. X. (1996) *J. Biol. Inorg. Chem. 1*, 372−376.
25. Finzel, B. C., Poulos, T. L., and Kraut, J. (1984) *J. Biol. Chem. 259*, 13027−13036.
26. Poulos, T. L., Finzel, B. C., Gunsalus, I. C., Wagner, G. C., and Kraut, J. (1985) *J. Biol. Chem. 260*, 16122−16130.
27. Yeung, B. K., Wang, X., Sigman, J. A., Petillo, P. A., and Lu, Y. (1997) *Chem. Biol. 4*, 215−221.
28. Huff, A. M., Chang, C. K., Cooper, D. K., Smith, K. M., and Dawson, J. H. (1993) *Inorg. Chem. 32*, 1460−1466.
29. Andersson, L. A. (1982) *The Active Site Environments of Heme Mono-oxygenases: Spectroscopic Investigations of Cytochrome P450 and Secondary Amine Mono-oxygenase*, Ph.D. Thesis, University of South Carolina, Columbia, SC.
30. Dawson, J. H., Andersson, L. A., and Sono, M. (1982) *J. Biol. Chem. 257*, 3606−3617.
31. Dawson, J. H., Andersson, L. A., and Sono, M. (1992) *New J. Chem. 16*, 577−582.
32. Vickery, L., Salmon, A., and Sauer, K. (1975) *Biochim. Biophys. Acta 386*, 87−89.
33. Lipscomb, J. D. (1980) *Biochemistry 19*, 3590−3599.
34. Hollenberg, P. F., Hager, L. P., Blumberg, W. E., and Peisach, J. (1980) *J. Biol. Chem. 255*, 4801−4807.
35. Yonetani, T., and Anni, H. (1987) *J. Biol. Chem. 262*, 9547−9554.
36. Sono, M., Dawson, J. H., Hall, K., and Hager, L. P. (1986) *Biochemistry 25*, 347−356.
37. Erman, J. E. (1974) *Biochemistry 13*, 39−44.
38. Sono, M., Hager, L. P., and Dawson, J. H. (1991) *Biochim. Biophys. Acta 1078*, 351−359.
39. Collman, J. P., Sorrell, T. N., and Hoffman, B. M. (1975) *J. Am. Chem. Soc. 97*, 913−914.
40. Koch, S., Tang, S. C., Holm, R. H., Frankel, R. B., and Ibers, J. A. (1975) *J. Am. Chem. Soc. 97*, 916−918.
41. Koch, S., Tang, S. C., Holm, R. H., and Frankel, R. B. (1975) *J. Am. Chem. Soc. 97*, 914−916.
42. Poulos, T. L. (1996) *J. Biol. Inorg. Chem. 1*, 356−359.
43. Goodin, D. B. (1996) *J. Biol. Inorg. Chem. 1*, 360−363.
44. Sundaramoorthy, M., Terner, J., and Poulos, T. L. (1995) *Structure 3*, 1367−1377.
45. Ueno, T., Kousumi, Y., Yoshizawa-Kumagaye, K., Nakajima, K., Ueyama, N., Okamura, T.-a., and Nakamura, A. (1998) *J. Am. Chem. Soc. 120*, 12264−12273.
46. Cupp-Vickery, J. R., and Poulos, T. L. (1995) *Nat. Struct. Biol. 2*, 144−153.
47. Hasemann, C. A., Ravichandran, K. G., Peterson, J. A., and Deisenhofer, J. (1994) *J. Mol. Biol. 236*, 1169−1185.
48. Ravichandran, K. G., Boddupalli, S. S., Hasemann, C. A., Peterson, J. A., and Deisenhofer, J. (1993) *Science 261*, 731−736.
49. Goodin, D. B., and McRee, D. E. (1993) *Biochemistry 32*, 3313−3324.
50. Tang, S. C., Koch, S., Papaefthymiou, G. C., Foner, S., Frankel, R. B., Ibers, J. A., and Holm, R. H. (1976) *J. Am. Chem. Soc. 98*, 2414−2434.
51. Dawson, J. H., and Sono, M. (1987) *Chem. Rev. 87*, 1255−1276.
52. Tsai, R., Yu, C. A., Gunsalus, I. C., Peisach, J., Blumberg, W., Orme-Johnson, W. H., and Beinert, H. (1970) *Proc. Natl. Acad. Sci. U.S.A. 66*, 1157−1163.
53. Ozols, J., and Strittmatter, P. (1964) *J. Biol. Chem. 239*, 1018−1023.
54. Lloyd, E., Hildebrand, D. P., Tu, K. M., and Mauk, A. G. (1995) *J. Am. Chem. Soc. 117*, 6434−6438.
55. McKnight, J., Cheesman, M. R., Thomson, A. J., Miles, J. S., and Munro, A. W. (1993) *Eur. J. Biochem. 213*, 683−687.
56. Reynolds, M. F., Shelver, D., Kerby, R. L., Parks, R. B., Roberts, G. P., and Burstyn, J. N. (1998) *J. Am. Chem. Soc. 120*, 9080−9081.
57. Chevion, M., Peisach, J., and Blumberg, W. E. (1977) *J. Biol. Chem. 252*, 3637−3645.
58. Martinis, S. A., Sotiriou, C., and Chang, C. K. (1989) *Biochemistry 28*, 879−884.
59. Blumberg, W. E., Peisach, J., Wittenberg, B. A., and Wittenberg, J. B. (1968) *J. Biol. Chem. 243*, 1854−1862.
60. Chang, C. K., and Dolphin, D. (1975) *J. Am. Chem. Soc 20*, 5948−5950.
61. Yu, C.-A., and Gunsalus, I. C. (1974) *J. Biol. Chem. 249*, 94−101.
62. Hollenberg, P. F., and Hager, L. P. (1973) *J. Biol. Chem. 248*, 2630−2633.
63. Griffin, B. W., Peterson, J. A., and Estabrook, R. W. (1979) in *The Porphyrins* (Dolphin, D., Ed.) Vol. 7, pp 333−375, Academic Press, New York.
64. Shiro, Y., Fujii, M., Isogai, Y., Adachi, S.-i., Iizuka, T., Obayashi, E., Makino, R., Nakahara, K., and Shoun, H. (1995) *Biochemistry 34*, 9052−9058.

BI990815O